

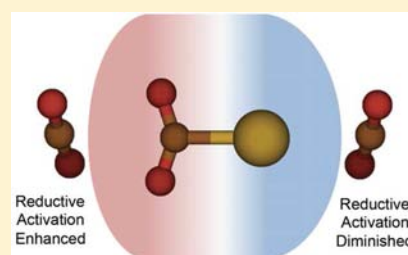
# Solvent-Driven Reductive Activation of Carbon Dioxide by Gold Anions

Benjamin J. Knurr and J. Mathias Weber\*

JILA, NIST, and Department of Chemistry and Biochemistry, University of Colorado at Boulder, Boulder, Colorado 80309-0440, United States

**S** Supporting Information

**ABSTRACT:** Catalytic activation and electrochemical reduction of CO<sub>2</sub> for the formation of chemically usable feedstock and fuel are central goals for establishing a carbon neutral fuel cycle. The role of solvent molecules in catalytic processes is little understood, although solvent–solute interactions can strongly influence activated intermediate species. We use vibrational spectroscopy of mass-selected Au(CO<sub>2</sub>)<sub>n</sub><sup>−</sup> cluster ions to probe the solvation of AuCO<sub>2</sub><sup>−</sup> as a model for a reactive intermediate in the reductive activation of a CO<sub>2</sub> ligand by a single-atom catalyst. For the first few solvent molecules, solvation of the complex preferentially occurs at the CO<sub>2</sub> moiety, enhancing reductive activation through polarization of the excess charge onto the partially reduced ligand. At higher levels of solvation, direct interaction of additional solvent molecules with the Au atom diminishes reduction. The results show how the solvation environment can enhance or diminish the effects of a catalyst, offering design criteria for single-atom catalyst engineering.



## INTRODUCTION

The development of dependable and sustainable energy sources is one of the most pressing issues of the early 21st century. Under the assumption that many areas of technology will continue to depend on the use of carbon based chemical fuels for the foreseeable future, environmental as well as economic pressures call for the development of carbon neutral fuel cycles. As a consequence, sequestration and recycling of CO<sub>2</sub> emitted from combustion of fuels is a major goal of catalysis research. Any scheme for the conversion of CO<sub>2</sub> into chemically usable fuels requires reduction, where the most simple reduction of CO<sub>2</sub> ending in the formation of formate anion (HCOO<sup>−</sup>) requires transfer of two electrons and one proton (see, e.g., ref 1). A recently developed promising avenue toward more complex products is an electrochemical approach to convert CO<sub>2</sub> to methanol in a six-electron reduction process using pyridine based homogeneous catalysts.<sup>2</sup> A key intermediate in this approach is the C<sub>3</sub>H<sub>5</sub>N-CO<sub>2</sub><sup>−</sup> anion, where the CO<sub>2</sub> molecule is covalently bound to a pyridinium anion. Many other approaches to similar catalytic processes involve metal based catalysts.<sup>3–7</sup> Particularly interesting in this context are single-atom or few-atom catalysts, where metal atoms or clusters<sup>8</sup> are supported on a surface or embedded in a binding site of a supramolecular assembly<sup>9</sup> or multiligand system.<sup>3,4,10</sup>

In the case of an isolated CO<sub>2</sub> molecule, even one-electron reduction is energetically expensive, requiring 0.6 eV per molecule, resulting in a metastable CO<sub>2</sub><sup>−</sup> anion.<sup>11</sup> Alternatively, a catalyst can transfer negative charge to a CO<sub>2</sub> molecule by forming a covalent bond with it. In this case, a fractional charge transfer will take place, reductively activating the CO<sub>2</sub> molecule for further reaction steps. Earlier work on the structure of simple binary anionic complexes of CO<sub>2</sub> and atomic gold<sup>12,13</sup>

revealed that CO<sub>2</sub> forms a covalent bond with Au<sup>−</sup> (binding energy ca. 0.4 eV<sup>12</sup>) with the excess charge partially transferred onto the CO<sub>2</sub> moiety of the nascent auryl formate complex, AuCO<sub>2</sub><sup>−</sup>. In this complex, the CO<sub>2</sub> ligand is strongly bent due to a partial charge calculated to be  $-0.47 e$ . Excess electronic charge in CO<sub>2</sub> is initially accommodated in antibonding CO  $\pi^*$  orbitals. As a result, the CO  $\pi$  bonds are weakened and the CO<sub>2</sub> molecule is distorted from its linear geometry in the neutral charge state to a bent configuration with an OCO bond angle of 143°. These changes in charge distribution can be probed by monitoring the vibrational modes in the reductively activated CO<sub>2</sub> molecule, where the CO stretching modes will progressively shift to lower frequencies as the CO bonds are increasingly weakened by charge transfer.

Among the less understood aspects of CO<sub>2</sub> reduction is the role of solvent in both homogeneous and heterogeneous catalysis, that is, how the interplay of solvent molecules with the catalyst and CO<sub>2</sub> affects the reduction process. The presence of solvent molecules can have profound effects on the charge distribution in ions,<sup>14,15</sup> as they can polarize the excess charge and even lead to changes in the structure and nature of the charge carrier.<sup>16,17</sup> It is therefore of great interest to study how solvent interacts with single-atom or few-atom metal catalysts during reduction of CO<sub>2</sub>, as these effects will inevitably be present in electrochemical applications.

Solvent effects are difficult to probe in detail in the condensed phase, due to the unavoidable fluctuations in the solvation environment and the lack of control over the number of solvent molecules interacting with a solute. Gas phase cluster

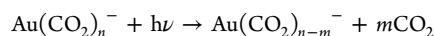
Received: September 10, 2012

Published: October 25, 2012

studies have proven to be a highly valuable tool for the understanding of ion solvation. In particular, vibrational spectroscopy of mass selected cluster ions affords precise control over the composition and size of the solvation environment together with a sensitive probe of the local structure of solvent and solute.<sup>18–23</sup> For the case of CO<sub>2</sub> bound to a negative ion, the antisymmetric stretching vibration provides a convenient probe to track the level of deformation and reductive activation of CO<sub>2</sub>. Here, we focus on the structural and electronic changes that occur in a complex of CO<sub>2</sub> bound to a gold anion as the complex is solvated by additional CO<sub>2</sub> molecules, which would be relevant, for example, in reduction processes in supercritical CO<sub>2</sub>.<sup>24</sup>

## METHODS

**Experimental.** Our experimental setup is based on ideas by Lineberger and co-workers<sup>25</sup> and has been described elsewhere in detail.<sup>26–28</sup> Briefly, Au(CO<sub>2</sub>)<sub>n</sub><sup>−</sup> ions were generated combining laser vaporization of a gold target and electron impact ionization of a pulsed expansion of neat CO<sub>2</sub> (Even-Lavie valve, stagnation pressure 5.5 bar).<sup>28</sup> Ions were mass separated in a Wiley–McLaren type time-of-flight mass spectrometer. In the first space focus of the mass spectrometer, the ions of interest were mass selected using a pulsed mass gate and irradiated with the pulsed output of an optical parametric converter (LaserVision) capable of producing infrared radiation in the wavenumber range 600–4000 cm<sup>−1</sup>. Fragments were formed upon photon absorption by evaporation of solvent CO<sub>2</sub> molecules:



Fragment ions were separated from parent ions using a two-stage reflectron and detected on a dual microchannel plate detector. Infrared spectra were measured by monitoring the fragment ion signal as a function of wavenumber. The ion signals were corrected for infrared fluence. The experiment was repeated on different days for each ion species to ensure reproducibility and several scans were averaged for each spectrum to increase the signal-to-noise ratio.

**Computational.** We employed density functional theory (B3-LYP functional with dispersion correction,<sup>29</sup> TZVPP basis sets for all atoms) to obtain structures, relative energies, natural population analysis and vibrational spectra of low energy conformers of Au(CO<sub>2</sub>)<sub>n</sub><sup>−</sup> cluster ions for  $n = 1–5$  using the TURBOMOLE suite of programs<sup>30</sup> (V.5.9.1 and V.6.2). Infrared spectra of the conformers were calculated with the AOFORCE program. All conformers reported here are minima on the potential energy surface. Predicted infrared frequencies for each conformer were obtained from harmonic approximation calculations and multiplied by a factor of 0.9380 to account for anharmonicity. This factor was obtained by comparing the harmonic approximation values for AuCO<sub>2</sub><sup>−</sup> from the present calculations with the anharmonic calculation by Boese et al.<sup>12</sup> Partial charges for low-energy conformers with preferential solvation of the reduced CO<sub>2</sub> moiety in Au(CO<sub>2</sub>)<sub>n</sub><sup>−</sup> ( $n = 1–5$ ) have been calculated using natural population analysis. We note that exploratory calculations using a more diffuse basis (aug-cc-pVTZ) for  $n = 2, 3$  yielded very similar structures, calculated infrared spectra and natural populations as the TZVPP calculations. Exploratory calculations for the same cluster sizes using the PBE0 functional also resulted in similar structures and infrared spectra. The magnitude of the PBE0 calculated negative charges on the reduced CO<sub>2</sub> ligand was somewhat higher, but followed the same trend as in the dispersion corrected B3-LYP calculations reported here.

## RESULTS AND DISCUSSION

Different from the related case of the pyridinium–CO<sub>2</sub> anion complex, where chemical intuition suggests that solvation will occur preferentially on the carboxylate group,<sup>31</sup> the solvation behavior of the auryl formate complex is not *a priori* clear. In

principle, solvent molecules could prefer the Au or the CO<sub>2</sub> moiety of the complex as binding sites. The consequences of these two scenarios for reductive activation are very different. Preferential solvation at the Au atom would polarize charge away from the activated CO<sub>2</sub> ligand. This would be unfavorable to CO<sub>2</sub> reduction and manifest itself in a blue shift of the antisymmetric stretching vibration of the partially reduced CO<sub>2</sub> ligand ( $\nu_r$ ). In contrast, solvation at the CO<sub>2</sub> side of the complex would accumulate more charge density on the CO<sub>2</sub> moiety of the complex. This would result in a stronger activation of the ligand, leading to a red shift of  $\nu_r$ .

Figure 1 shows a series of infrared spectra of mass selected Au(CO<sub>2</sub>)<sub>n</sub><sup>−</sup> cluster anions ( $n = 2–13$ ) in the region of the

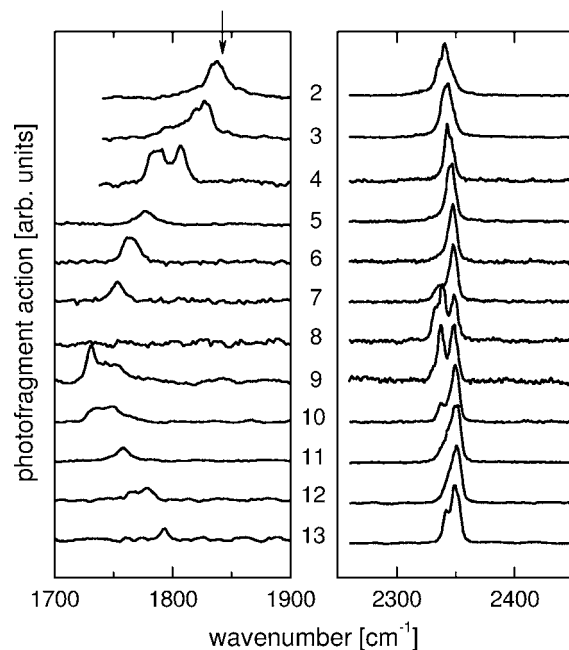


**Figure 1.** Infrared photodissociation spectra of Au(CO<sub>2</sub>)<sub>n</sub><sup>−</sup> cluster ions. Left panel: Signatures of the antisymmetric stretching vibration  $\nu_r$  of a partially reduced CO<sub>2</sub> ligand. The arrow in the top trace indicates  $\nu_r$  for  $n = 1$ .<sup>12</sup> Right panel: Signatures of the antisymmetric stretching vibrations  $\nu_{\text{solv}}$  of solvent CO<sub>2</sub> ligands. Numbers in the center denote the total number of CO<sub>2</sub> molecules in the cluster for each spectrum.

antisymmetric stretching vibration of the CO<sub>2</sub> ligands. The spectral region around 2350 cm<sup>−1</sup> contains the signatures of the weakly perturbed CO<sub>2</sub> solvent molecules ( $\nu_{\text{solv}}$ ), close to the antisymmetric stretching vibration of free CO<sub>2</sub> found at 2349 cm<sup>−1</sup>.<sup>32</sup> The signature  $\nu_r$  of the reductively activated CO<sub>2</sub> ligand bound covalently to the gold moiety is found between 1700 and 1850 cm<sup>−1</sup> for all cluster sizes under study and is strongly affected by solvation.

For  $n = 2–7$  and  $n = 9$ ,  $\nu_r$  signatures exhibit a clear, progressive red shift of  $(-13 \pm 3)$  cm<sup>−1</sup> per solvent molecule (see Figure 1), indicating that the activated CO<sub>2</sub> ligand is preferentially solvated in this size region. For  $n \geq 10$ , this trend is reversed, suggesting that additional CO<sub>2</sub> solvent molecules interact with the Au moiety of the auryl formate complex. We emphasize that solvation initially occurs on the reduced CO<sub>2</sub> ligand, increasing reductive activation.

Calculated low-energy conformers of Au(CO<sub>2</sub>)<sub>n</sub><sup>−</sup> clusters confirm the empirical interpretation above. Figure 2 shows the lowest energy structures of Au(CO<sub>2</sub>)<sub>n</sub><sup>−</sup> for  $n = 1–3$ . On the basis of these calculated structures, we can attribute the

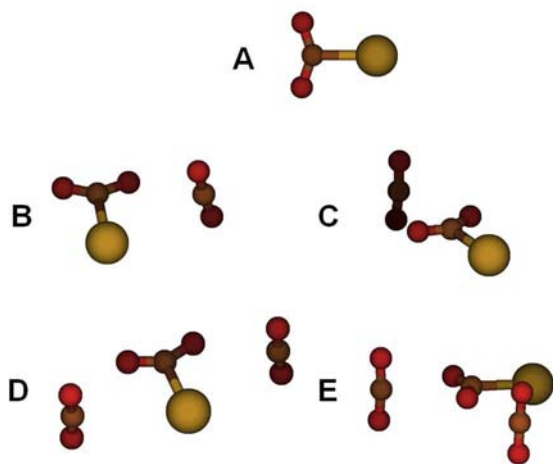


**Figure 2.** Calculated structures assigned to the experimental spectra of  $\text{Au}(\text{CO}_2)_n^-$  for  $n = 1-3$ . (A)  $n = 1$ ; (B and C) conformers for  $n = 2$ ; (D and E) conformers for  $n = 3$ . The calculated energies for conformer pairs B/C and D/E differ by less than 10 meV and are to be seen as isoenergetic. See Supporting Information for additional information on calculated structural conformers.

substructure in the  $\nu_r$  signatures to the population of several similar conformers where solvation occurs at the reduced  $\text{CO}_2$  ligand, but with slightly different arrangements of the solvent molecules. None of the low-lying calculated structures exhibit two strongly bound ligands, so the additional  $\text{CO}_2$  molecules (beyond the first  $\text{CO}_2$  ligand) act as solvent for the  $\text{AuCO}_2^-$  complex.

The predicted infrared spectra for the calculated low energy conformers for  $n = 2$  show a difference of ca.  $40 \text{ cm}^{-1}$ , and the higher calculated frequency is in better agreement with the experiment (see Figure 3). This frequency corresponds to the conformer shown in Figure 2B, where the solvent molecule is

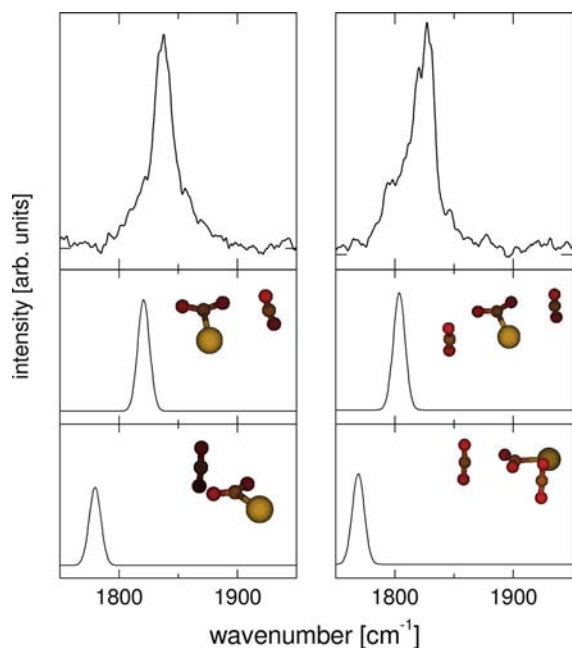


**Figure 3.** Experimental spectra (top traces) for  $n = 2$  (left) and  $n = 3$  (right) and predicted infrared spectra of the lowest energy conformers for these sizes (see text).

preferentially arranged between the reduced  $\text{CO}_2$  moiety and the Au atom of the solute ion, but closer to the  $\text{CO}_2$  group. We will refer to this binding site as the “side” position.

The experimental spectrum for  $n = 3$  shows an intense peak at  $1827 \text{ cm}^{-1}$  and a shoulder at  $1795 \text{ cm}^{-1}$ . The higher energy peak is consistent with the predicted spectrum of the conformer shown in Figure 2D, with both solvent molecules arranged between the Au atom and the reduced  $\text{CO}_2$ . The lower energy peak is consistent with the structure shown in Figure 2E, where the second solvent is only attached to the reduced  $\text{CO}_2$  moiety (“terminal” position), resulting in a stronger polarization of the charge, concomitant with a more pronounced red shift of  $\nu_r$ . For  $n = 4$ , several low-lying conformations give rise to two spectral signatures that recover the experimentally observed splitting (see Supporting Information Figure S3). Again, the higher frequency component corresponds to a conformer with the terminal position unoccupied, while conformers with ligands in the terminal position give rise to the lower frequency component. The calculated OCO bond angles for the partially reduced  $\text{CO}_2$  ligand range from  $140.7-142.7^\circ$  for  $n = 2$  to  $139-140^\circ$  for  $n = 5$ . The geometries of the solvent  $\text{CO}_2$  ligands are only minimally perturbed with bond angles of  $175-178^\circ$  (see Supporting Information).

For larger clusters (up to  $n = 9$ ), the reductively activated  $\text{CO}_2$  ligand continues to be the dominant binding site (except  $n = 8$ , see below). Following the size dependence of the experimentally observed values for  $\nu_r$ , we find that two sets of infrared signatures evolve (see Figure 4). Guided by the

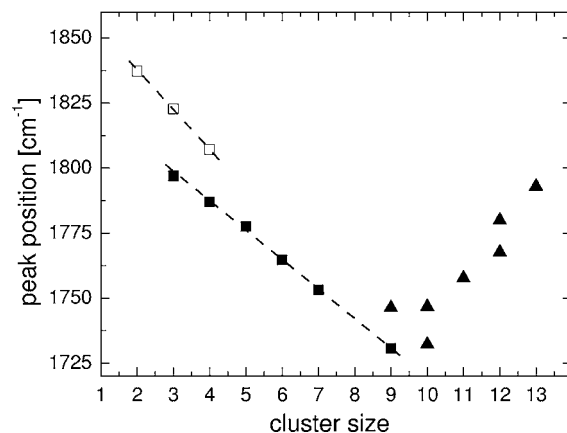


**Figure 4.** Cluster size dependence of the signature  $\nu_r$  of the reduced  $\text{CO}_2$  ligand. The symbols represent the experimental data, the dashed lines are meant to guide the eye. Open squares, terminal position unfilled; full squares, terminal position filled; triangles, solvation on Au moiety.

structural motifs identified for  $n = 3$  and  $n = 4$ , we attribute the lower energy series to a more efficiently solvated reduced ligand where the terminal position is occupied. We expect that both side and terminal positions are filled for  $n \geq 5$ . This results in a simpler spectrum with just a single peak in the  $\nu_r$  spectral region up to  $n = 7$ . For larger sizes, other effects resulting in the population of conformers with different solvation motifs are at play, causing a deviation from this simple picture.

The spectrum for  $n = 8$  is interesting as it lacks the signature of a reduced  $\text{CO}_2$  ligand. This can be explained by a switch in the charge carrier concomitant with closing the first solvation shell of  $\text{Au}^-$ , based on solvent shell closures observed in the same size range for similarly sized halide ions.<sup>33</sup> This change is

driven by the balance between the stability of the solute ion, its solvation energy and the size of its solvation shell. A more compact charge carrier has a more favorable solvation energy, but a smaller solvation shell. As the number of solvent molecules grows beyond the first solvation shell, it can be energetically more favorable to switch to a larger charge carrier and thereby enable more solvent molecules to directly solvate the charge. A similar change in the nature of the charge carrier has been observed previously<sup>16,17</sup> for neat  $(\text{CO}_2)_n^-$  cluster ions, where the charge carrier changes from  $(\text{CO}_2)_2^-$  to  $\text{CO}_2^-$  at  $n = 6$  and back to  $(\text{CO}_2)_2^-$  at  $n = 14$ . Our results for  $\text{Au}(\text{CO}_2)_n^-$  clusters suggest that  $\text{Au}^-$  as a charge carrier is favorable only at the cluster size where its first solvent shell is closed ( $n = 8$ ), explaining the absence of the signature of a reduced ligand for that cluster size.

On the basis of the trend of the lower energy feature in the  $\nu_r$  spectral region as a function of cluster size, we judge that the addition of solvent molecules on the reduced  $\text{CO}_2$  ligand continues up to  $n = 9$ . At this size, the partial solvent shell around the reduced ligand is filled, so that additional solvent molecules will begin to solvate the Au moiety of the  $\text{AuCO}_2^-$  solute ion. This results in a blue shift of  $\nu_r$  and we assign the higher energy feature in the  $\nu_r$  spectral region of  $n = 9$  to be the first signature of this change in the solvation motif, which continues for larger clusters.

For catalytic  $\text{CO}_2$  reduction, the charge on the activated ligand is an important figure of merit. Combining computational population analysis and the observed experimental red shift allows us to estimate the amount of charge transfer to the reduced  $\text{CO}_2$  moiety. Figure 5 shows  $\nu_r$  as a function of the

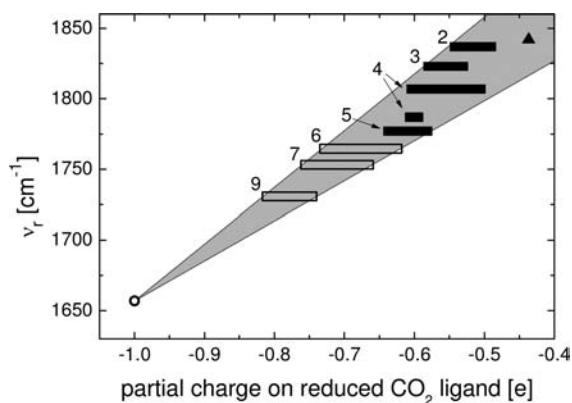


**Figure 5.** Effects of partial charge on the antisymmetric stretching mode  $\nu_r$  of the reduced  $\text{CO}_2$  ligand for different cluster sizes  $n$  (shown as numbers). Triangle: Anharmonic prediction of  $\nu_r$  in bare  $\text{AuCO}_2^-$ .<sup>12</sup> Circle: Antisymmetric stretching mode of  $\text{CO}_2^-$  in a Ne matrix.<sup>34</sup> Solid bars: Range of calculated partial charges for the given cluster sizes, together with their experimental values for  $\nu_r$  (see Figure 1). Open bars: Extrapolated range of partial charges for the given cluster sizes, based on the  $\text{CO}_2^-$  data and the envelope of the calculated charges (gray shaded area).

calculated charge transfer. The limiting case is given by the  $\text{CO}_2^-$  anion, which has an excess charge  $-e$  and shows its antisymmetric stretching mode at  $1658.3 \text{ cm}^{-1}$ .<sup>34</sup> On the basis of calculated partial charges from a natural population analysis of small cluster ions ( $n = 1-5$ ), we can estimate the charge transfer in larger clusters. For the cluster size with the lowest value of  $\nu_r$  ( $n = 9$ ), we arrive at an estimate around  $-0.8 e$  for the partial charge on the reduced  $\text{CO}_2$  ligand. This constitutes a

significant solvent-driven enhancement in reductive activation compared to the case of  $\text{AuCO}_2^-$  ( $-0.47 e$ ).

In contrast to  $\nu_r$ , variations in  $\nu_{\text{solv}}$  with increasing cluster size are rather small. The spectral region covering the antisymmetric stretching mode of solvent  $\text{CO}_2$  molecules shows peaks which are weakly red-shifted from the antisymmetric  $\text{CO}_2$  stretching mode of free  $\text{CO}_2$ . The different peaks distinguishable in some of the spectra highlight the existence of structurally inequivalent solvent molecules with similar roles. For example, a solvent molecule interacting with the Au atom has slightly different  $\nu_{\text{solv}}$  than one interacting with the reduced  $\text{CO}_2$  ligand. The observation of several peaks in the  $\nu_{\text{solv}}$  region indicates that the solvent shell has low symmetry, even in the case of  $n = 8$ .

## CONCLUSIONS

Our results unambiguously show that the interaction of solvent molecules with reactive intermediates involving polarizable charge distributions can have strong effects on the degree of reduction of a molecular ligand. In this context, our results offer suggestions for the design of single-atom metal catalysts for solvent driven reductive activation of  $\text{CO}_2$ . Since only the first few solvent molecules enhance charge transfer onto the  $\text{CO}_2$  moiety, reductive activation of  $\text{CO}_2$  can be improved by allowing solvent access to the partially reduced ligand, but sterically hindering direct interaction between the metal catalyst and the solvent.

## ASSOCIATED CONTENT

### Supporting Information

Calculated structures and spectra of low energy conformers of  $\text{Au}(\text{CO}_2)_n^-$  cluster ions for  $n = 2-5$ . This material is available free of charge via the Internet at <http://pubs.acs.org>.

## AUTHOR INFORMATION

### Corresponding Author

[weberjm@jila.colorado.edu](mailto:weberjm@jila.colorado.edu)

### Notes

The authors declare no competing financial interest.

## ACKNOWLEDGMENTS

We gratefully acknowledge funding from the National Science Foundation under grant number CHE-0845618.

## REFERENCES

- (1) Hori, Y. Electrochemical  $\text{CO}_2$  Reduction on Metal Electrodes. In *Modern Aspects of Electrochemistry*; Vayenas, C. G., White, R. E., Gamboa-Aldeco, M. E., Eds.; Springer: New York, 2008; Vol. 42, pp 89–189.
- (2) Cole, E. B.; Lakkaraju, P. S.; Rampulla, D. M.; Morris, A. J.; Abelev, E.; Bocarsly, A. B. *J. Am. Chem. Soc.* **2010**, *132*, 11539–11551.
- (3) Tanaka, K.; Ooyama, D. *Coord. Chem. Rev.* **2002**, *226*, 211–218.
- (4) Bian, Z. Y.; Sumi, K.; Furue, M.; Sato, S.; Koike, K.; Ishitani, O. *Inorg. Chem.* **2008**, *47*, 10801–10803.
- (5) Inagaki, A.; Akita, M. *Coord. Chem. Rev.* **2010**, *254*, 1220–1239.
- (6) Khenkin, A. M.; Efremenko, I.; Weiner, L.; Martin, J. M. L.; Neumann, R. *Chem.—Eur. J.* **2010**, *16*, 1356–1364.
- (7) Doherty, M. D.; Grills, D. C.; Muckerman, J. T.; Polyansky, D. E.; Fujita, E. *Coord. Chem. Rev.* **2010**, *254*, 2472–2482.
- (8) Heiz, U.; Bullock, E. L. *J. Mater. Chem.* **2004**, *14*, 564–577.
- (9) Oosterom, G. E.; Reek, J. N. H.; Kamer, P. C. J.; van Leeuwen, P. *Angew. Chem., Int. Ed.* **2001**, *40*, 1828–1849.
- (10) Kauffman, D. R.; Alfonso, D.; Matranga, C.; Qian, H. F.; Jin, R. *J. Am. Chem. Soc.* **2012**, *134*, 10237–10243.

- (11) Knapp, M.; Echt, O.; Kreisler, D.; Mark, T. D.; Recknagel, E. *Chem. Phys. Lett.* **1986**, *126*, 225–231.
- (12) Boese, A. D.; Schneider, H.; Gloess, A. N.; Weber, J. M. *J. Chem. Phys.* **2005**, *122*, 154301–154301, through 154301–154307.
- (13) Kimble, M. L.; Castleman, A. W.; Mitric, R.; Burgel, C.; Bonacic-Koutecky, V. *J. Am. Chem. Soc.* **2004**, *126*, 2526–2535.
- (14) Schneider, H.; Weber, J. M. *J. Chem. Phys.* **2007**, *127*, 244310.
- (15) Marcum, J. C.; Weber, J. M. *J. Phys. Chem. A* **2010**, *114*, 8933–8938.
- (16) Tsukuda, T.; Johnson, M. A.; Nagata, T. *Chem. Phys. Lett.* **1997**, *268*, 429–433.
- (17) Shin, J. W.; Hammer, N. I.; Johnson, M. A.; Schneider, H.; Glöss, A.; Weber, J. M. *J. Phys. Chem. A* **2005**, *109*, 3146–3152.
- (18) Roscioli, J. R.; McCunn, L. R.; Johnson, M. A. *Science* **2007**, *316*, 249–254.
- (19) Duncan, M. A. *Int. Rev. Phys. Chem* **2003**, *22*, 407–435.
- (20) Miyazaki, M.; Fujii, A.; Ebata, T.; Mikami, N. *Science* **2004**, *304*, 1134–1137.
- (21) Shin, J. W.; Hammer, N. I.; Diken, E. G.; Johnson, M. A.; Walters, R. S.; Jaeger, T. D.; Duncan, M. A.; Christie, R. A.; Jordan, K. D. *Science* **2004**, *304*, 1137–1140.
- (22) Relph, R. A.; Guasco, T. L.; Elliott, B. M.; Kamrath, M. Z.; McCoy, A. B.; Steele, R. P.; Schofield, D. P.; Jordan, K. D.; Viggiano, A. A.; Ferguson, E. E.; Johnson, M. A. *Science* **2010**, *327*, 308–312.
- (23) Garand, E.; Kamrath, M. Z.; Jordan, P. A.; Wolk, A. B.; Leavitt, C. M.; McCoy, A. B.; Miller, S. J.; Johnson, M. A. *Science* **2012**, *335*, 694–698.
- (24) Coates, G. W.; Moore, D. R. *Angew. Chem., Int. Ed.* **2004**, *43*, 6618–6639.
- (25) Johnson, M. A.; Lineberger, W. C. In *Techniques for the Study of Gas-Phase Ion Molecule Reactions*; Farrar, J. M., Saunders, W., Eds.; Wiley: New York, 1988; p 591.
- (26) Weber, J. M.; Schneider, H. *J. Chem. Phys.* **2004**, *120*, 10056.
- (27) Schneider, H.; Vogelhuber, K. M.; Weber, J. M. *J. Chem. Phys.* **2007**, *127*, 114311.
- (28) Weber, J. M. *Rev. Sci. Instrum.* **2005**, *76*, 043301.
- (29) Grimme, S. *J. Comput. Chem.* **2004**, *25*, 1463–1473.
- (30) Ahlrichs, R.; Bär, M.; Häser, M.; Horn, H.; Kölmel, C. *Chem. Phys. Lett.* **1989**, *162*, 165–169.
- (31) Kamrath, M. Z.; Relph, R. A.; Johnson, M. A. *J. Am. Chem. Soc.* **2010**, *132*, 15508–15511.
- (32) Herzberg, G. *Molecular Spectra and Molecular Structure*; Krieger Publishing Co.: Malabar, FL, 1991; Vol. III.
- (33) Arnold, D. W.; Bradforth, S. E.; Kim, E. H.; Neumark, D. M. *J. Chem. Phys.* **1995**, *102*, 3510–3518.
- (34) Thompson, W. E.; Jacox, M. E. *J. Chem. Phys.* **1999**, *111*, 4487–4496.